To check that the coatings were both rugged and chemically inert, several devices were submerged in water for an hour. Their reflectivity was remeasured and found not to have changed within the resolution of our measurement (±0·5 dB). The coatings were similarly unaffected by further processing with several cleans of concentrated fuming nitric acid.

Conclusions: We have described a novel ion-assisted deposition technique which allows large numbers of rugged, chemically inert coatings to be deposited at low temperature on lithium niobate devices. Measurements have shown that devices may be produced with low reflectivities, in agreement with theory. In particular, a device with a reflectivity to air of −42 dB, for TM-polarised light at 1·55 μm, was produced with a silicon dioxide coating. The technique is applicable to a range of coating materials.

Acknowledgment: We thank A. R. Beaumont, R. C. Booth, M. C. Brain, A. M. C. Carden, G. P. Markham, A. P. Thomas, N. G. Walker and P. J. Zirngast for their assistance. We also thank BT&D Technologies for sponsorship, and the Director of Research & Technology, British Telecom for permission to publish this letter.

J. DAVIDSON
I. REID

British Telecom Research Laboratories
Martlesham Heath
Ipswich IP5 7RE, United Kingdom

3rd January 1989

References

1 CREANER, M. J., *et al.*: '565 Mbit/s DPSK heterodyne transmission system experiment using packaged external cavity and a lithium niobate polarisation controller'. Proc. ECOC 1988, Sept. 1988, **1**, pp. 179–182
2 PRESTON, K. R., *et al.*: 'High performance hermetic package for lithium niobate electrooptic waveguide devices'. Proc. optoelectronics materials, devices, packaging and interconnects II conf., Sept. 1988
3 RAO, R., and COOK, J. S.: 'High return loss connector design without using fibre contact or index matching', *Electron. Lett.*, 1986, **22**, pp. 731–732
4 EISENSTEIN, G., KOROTKY, S. K., STULZ, L. W., VESELKA, J. J., JOPSON, R. M., and HALL, K. L.: 'Antireflection coatings on lithium niobate waveguide devices using electron beam evaporated yttrium oxide', *ibid.*, 1985, **21**, pp. 363–364
5 MACLEOD, H. A.: 'Overview of coating techniques', *Proc. SPIE*, 1984, **476**, pp. 128–135
6 MARTIN, P. J., MACLEOD, H. A., NETTERFIELD, R. P., PACEY, C. G., and AINTY, W. G. S.: 'Ion beam assisted deposition of thin films', *Appl. Opt.*, 1983, **22**, p. 178
7 WANG, J.: 'New method to measure facet reflectivity of antireflection (AR)-coated laser diodes and LEDs', *Electron. Lett.*, 1985, **21**, pp. 929–931
8 DOBROWOLSKI, J. A.: 'Handbook of optics' (McGraw-Hill, 1978), Sec. 8
9 NELSON, D. F., and MIKULYAK, R. M.: 'Refractive indices of congruently melting lithium niobate', *J. Appl. Phys.*, 1974, **45**, p. 3688

5·5 GHz MULTIPLE QUANTUM WELL REFLECTION MODULATOR

Indexing terms: Optoelectronics, Optical modulation, Modulators, Quantum optics

We report the fabrication and operation of a high-speed reflection modulator using the quantum-confined Stark effect in GaAs quantum wells grown over a dielectric mirror. The modulator has a 5·5 GHz 3 dB response.

Optical modulators based on the quantum-confined Stark effect electroabsorption in quantum wells have been demonstrated in a number of materials systems, both in mesa configurations in which the light propagates perpendicular to the surface and in waveguides with the light propagating in the plane of the quantum well layers[1] with devices operating in the GHz regime.[2–7] Recently we demonstrated a mesa modulator diode structure grown on top of a quarter-wave dielectric stack mirror fabricated in the same growth run, all in GaAs/AlGaAs.[8] The double pass of the incident light through the quantum wells improves the modulator contrast, and the GaAs substrate (which is opaque at the operating wavelength) need not be removed. This simple structure also allows high-speed electrical mounting techniques developed for laser diodes or photodetectors, and in this letter we report a modulator with a 5·5 GHz bandwidth, the fastest so far reported for a quantum well modulator in any configuration to our knowledge.

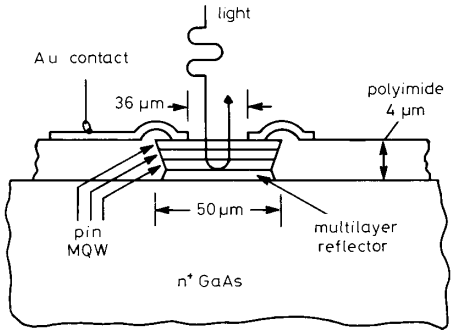

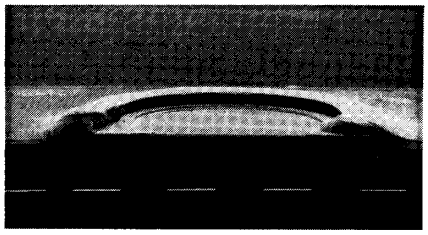

907/1

Fig. 1 *High-speed MQW modulator, showing pin MQW modulator grown on multilayer (12 pairs of alternate λ/4-thick layers) reflector*
Also shown is SEM photograph of cleaved mesa device

Fig. 1 shows the present device fabricated from portions of the previous wafer.[8] The smallest device was a circular mesa of 50 μm diameter which was covered with a polyimide layer 4 μm thick in which a 44 μm-diameter hole centred on the mesa was etched. A gold pad 100 × 150 μm was fabricated by liftoff, leaving a 36 μm-diameter window over the mesa. An antireflection layer of SiO_2 was deposited in the window and over the exposed polyimide. This polyimide technique for the reduction of parasitic capacitance has been used recently in semiconductor devices.[9] The modulators were connected, using wires several hundred microns long, to a Wiltron microstrip-to-'K' connector adapter.

The response of this device was measured in the frequency domain with an HP8510 network analyser plus amplifiers to apply a swept microwave signal to a bias 'T'. The network analyser delivers constant output power (not voltage) to the modulator. The bias voltage ranged from 0 to −20 V, and the RF signal was up to 1 V peak. The optical beam was from a Kr-ion-laser-pumped Styryl-9 dye laser set to the heavy hole exciton absorption at 853 nm.[8] A lens focuses the laser beam on the device to ~10 μm and also forms an optical microscope so that the device and the beam can be observed using a CCD camera. The reflected modulated light was detected on an Ortel PD025 GaAs photodiode. The RF signal from the detector passed through another bias 'T' to an amplifier and back to the network analyser. The frequency responses of the photodiode, the cables and the amplifiers were separately calibrated using 1 ps laser pulses from another source.[10] Frequency scans of the modulator were from 45 MHz to 2 GHz and from 2 to 6 GHz.

Two different-sized mesa modulators were measured and, after subtracting the response of the photodiode, the frequency response is shown in Fig. 2. We observed 3 dB electri-

cal frequency response bandwidths of 4 and 5·5 GHz for the 100 and 50 μm mesas, respectively. If the modulator is modelled as a simple series RC circuit in which the response is proportional to the voltage across the capacitor, then the electrical response (ER) is given by

$$ER = 10 \log [1 + (f/f_c)^2] \quad (1)$$

$$f_c = 1/2\pi RC \quad (2)$$

The response of this RC model circuit is also plotted in Fig. 2 for several values of f_c. The response seems to drop faster than a simple RC for both mesas; despite various attempts we have not devised a more complex model for the circuit that explains this. The optical response of the modulator in dB is one half of the electrical response in Fig. 2. The frequency response cutoff is listed in Table 1, and an equivalent time constant $\tau_c = RC$ calculated from eqn. 1 and low-frequency C measurements given.

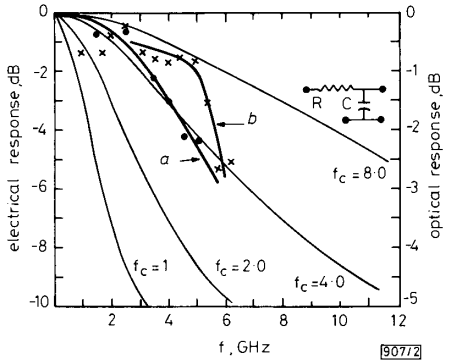

Fig. 2 *Electrical response of MQW modulator of mesa diameters (a) 100 μm and (b) 50 μm*

Curves labelled as to f_c are from simple RC model as given by eqns. 1 and 2

The total capacitance is the sum of the mesa capacitance and the gold pad capacitance. The Au pad is 150 × 100 μm over polyimide 2–4 μm thick, but on the smaller device (50 μm diameter) the Ag epoxy spilled over on the polyimide and doubled the pad area. The epoxy of the larger mesa did not spill over. A simple calculation using the total capacitance and the fact that the larger mesa is four times the area of the smaller mesa indicates a pad capacitance of $C_p = 0{\cdot}15$ and 0·30 pF, respectively, and mesa capacitance C_m of 0·68 and 0·17 pF for the 100 and 50 μm mesas, respectively, giving a mesa capacitance of $0{\cdot}87 \times 10^{-16}$ F/μm^2. Theory calculates for our[8] 1·0 μm-thick MQW structure at zero bias a capacitance of $1{\cdot}03 \times 10^{-16}$ F/μm^2. Experiment and theory show an approximate 10–15% decrease in capacitance at a reverse bias of 10 V, which reduces the calculated value to close agreement with the above measurement of $0{\cdot}87 \times 10^{-16}$ F/μm^2. For the polyimide of thickness 4 μm and $\kappa = 3{\cdot}5$, the pad capacitance C_p for the gold area calculates as 0·12 pF, in good agreement with the inferred value of 0·15 pF.

Taking the measured f_c (and $\tau_c = 1/2\pi f_c$) and assuming that all the capacitance, $C = C_p + C_m$, is charged through a single resistance $R_{equiv} = \tau_c/C$, gives the values of R_{equiv} in Table 1, which is consistent with a 50 Ω impedance being dominant in charging the capacitance.

Table 1

	Mesa diameter	
	(*a*) 100 μm	(*b*) 50 μm
f_c, GHz	4·0	5·5
τ_c, ps	40	29
C, pF	0·835	0·474
C_m, pF	0·68	0·17
C_p, pF	0·15	0·30
$R_{equiv} = \tau_c/C$, Ω	48	61

Total capacitance C was measured at 15 MHz and $V_b = -10$ V. Voltage dependence of C was less than 10% over 0 to −20 V range

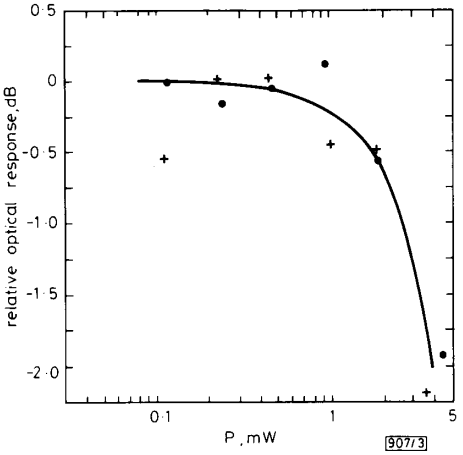

Fig. 3 *Relative electrical response (dB) against optical power on sample (b), with 50 μm mesa and 36 μm window*

$V_b = -10$ V
● 45 MHz + 2 GHz

The dependence of the modulation efficiency on incident optical power is shown in Fig. 3, the same at both 45 MHz and 2 GHz. The intensity level corresponding to the peak power level of 3·4 mW is approximately 4 kW/cm^2 assuming a 10 μm-diameter beam. For optical power above 2 mW the modulated output saturates. A possible cause is absorption saturation of the exciton absorption peak because of the optically created carrier density in the quantum wells.[11] This saturation starts at much higher intensities (~2·5 kW/cm^2) than that observed in unbiased quantum wells, which is consistent with the bias field sweeping the carriers out of the wells, thus reducing the effective carrier lifetime. When the modulation efficiency is saturating, the relative frequency response remains unchanged in our measurements, however. Further experiments and fabrication is required to find the ultimate limit of the frequency response of these MQW devices beyond 5·5 GHz.

We are indebted to our colleagues W. H. Knox and T. Sizer for their mode-locked lasers used to calibrate the frequency response of the detector, and T. H. Wood, A. R. Chraplyvy, R. S. Tucker and T. L. Koch for discussion of measurement techniques. M. D. Feuer collaborated on the impedance measurements, and D. J. Burrows assisted with the experiments.

G. D. BOYD
J. E. BOWERS*
C. E. SOCCOLICH
D. A. B. MILLER
D. S. CHEMLA
L. M. F. CHIROVSKY
A. C. GOSSARD*
J. H. ENGLISH*

AT&T Bell Laboratories
Holmdel, NJ 07733, USA

28th November 1988

* Now at University of California at Santa Barbara, CA 93106, USA

References

1 MILLER, D. A. B.: 'Quantum wells for optical information processing', *Opt. Eng.*, 1987, **26**, pp. 368–372
2 WOOD, T. H., BURRUS, C. A., MILLER, D. A. B., CHEMLA, D. S., DAMEN, T. C., GOSSARD, A. C., and WIEGMANN, W.: '131 ps optical modulation in semiconductor multiple quantum wells (MQWs)', *IEEE J. Quantum Electron.*, 1985, **QE-21**, pp. 117–118
3 KOREN, U., MILLER, B. I., TUCKER, R. S., EISENSTEIN, G., BAR-JOSEPH, I., MILLER, D. A. B., and CHEMLA, D. S.: 'High-frequency InGaAs/InP multiple-quantum-well buried-mesa electroabsorption optical modulator', *Electron. Lett.*, 1987, **23**, pp. 621–622
4 WOOD, T. H., CARR, E. C., BURRUS, C. A., TUCKER, R. S., CHIU, T.-H., and TSANG, W.-T.: 'High-speed waveguide optical modulator made

from GaSb/AlGaSb multiple quantum wells (MQWs)', *ibid.*, 1987, **23**, pp. 540–542
5 WOOD, T. H., BURRUS, C. A., TUCKER, R. S., WEINER, J. S., MILLER, D. A. B., CHEMLA, D. S., DAMEN, T. C., GOSSARD, A. C., and WIEGMANN, W.: '100 ps waveguide MQW optical modulator with 10:1 on/off ratio', *ibid.*, 1985, **21**, pp. 693–694
6 KOREN, U., MILLER, B. I., KOCH, T. L., EISENSTEIN, G., TUCKER, R. S., BAR-JOSEPH, I., and CHEMLA, D. S.: 'Low-loss InGaAs/InP multiple quantum well optical electroabsorption waveguide modulator', *Appl. Phys. Lett.*, 1987, **51**, pp. 1132–1133
7 MANNING, R. J., BRADLEY, P. J., MILLER, A., ROBERTS, J. S., MISTRY, P., and PATE, M.: 'Photoconductive response time of a multiple quantum well *pin* modulator', *Electron. Lett.*, 1988, **24**, pp. 854–855
8 BOYD, G. D., MILLER, D. A. B., CHEMLA, D. S., MCCALL, S. L., GOSSARD, A. C., and ENGLISH, J. H.: 'Multiple quantum well reflection modulator', *Appl. Phys. Lett.*, 1987, **50**, pp. 1119–1121
9 BOWERS, J. E.: 'High-speed semiconductor laser design and performance', *Solid-State Electron.*, 1987, **30**, pp. 1–11; BOWERS, J. E., and BURRUS, C. A.: 'Ultrawide-band long-wavelength PIN photodetectors', *J. Lightwave Technol.*, 1987, **LT-5**, pp. 1339–1350
10 KNOX, W. H.: 'Generation and kilohertz-rate amplification of femtosecond optical pulses around 800 nm', *J. Opt. Soc. Am. B*, Nov. 1987
11 CHEMLA, D. S., and MILLER, D. A. B.: 'Room temperature excitonic nonlinear optical effects in semiconductor quantum well structures', *ibid.*, 1987, **2**, pp. 1155–1173

CORRELATION OF TUNNELLING CURRENTS AND TUNABLE LUMINESCENCE IN SELECTIVELY DIFFUSED *nipi* LEDs

Indexing terms: Light-emitting diodes, Tunelling, Luminescence

Measurements of the current/voltage characteristics and electroluminescence spectra of *nipi* LEDs with selectively diffused contacts have been performed over the temperature range 3–300 K. Good correlation has been observed between the forward characteristics of the diodes and the tuning of the electroluminescence. Analysis of the I/V characteristics indicates that the recombination occurs by electron tunnelling through the parabolic potential barriers.

Doping superlattices (*nipi* structures) have recently been utilised in LEDs to provide tunable electroluminescence (EL).[1–3] The first structures utilised alloyed[1] and grown-in[2] contacts to the *n*- and *p*-layers of the doping superlattice. Recently we have reported on the use of selective diffusion to fabricate high-quality contacts to doping superlattices.[3] In this letter we correlate the electrical and spectral characteristics of LEDs fabricated by selective diffusion to identify the various components of current injection in the structures.

The GaAs *nipi* LEDs were fabricated from MBE-grown 10-layer doping superlattices with atomic doping levels of $n = p = 3 \times 10^{18}\,cm^{-3}$ and layer thicknesses $d_n = d_p = 300$ Å. Selective *p*- and *n*-diffusions separated by about 5 μm were used to fabricate the lateral injection structure, the details of which have been reported elsewhere.[3] The selective diffusion technique yields excellent selective contacts with a reverse breakdown voltage >9 V. The EL and I/V characteristics were compared over the temperature range 3–300 K.

The output spectrum of the LED at various drive voltages is shown in Fig. 1 at $T = 77$ K. The peak emission wavelength tunes over about 900 Å. The observable tuning range is limited in this case by the lower limit of our detection system, since there is little light output at the minimum drive currents of 30 μA. A plot of the spectral tuning characteristics of this device at various temperatures is shown in Fig. 2 over the temperature range 3–300 K. (The curves have been shifted by 30 meV intervals for clarity.) The inset shows the fitted tuning rates at various temperatures. At the low applied biases and at low temperatures (<100 K) the tuning of the output with bias is quite rapid and is temperature independent. At higher drive voltages the spectral output saturates near the band-gap energy which corresponds to nearly flat-band conditions in the *pn* junctions. The maximum tuning rate observed at low bias voltages is 0·7 eV/V. In an ideal system the change in emission energy would exactly equal the change in the applied voltage because of the position of the quasi-Fermi levels, but the rate is almost certainly limited in these structures by the high sheet resistance of the *p*-layers.

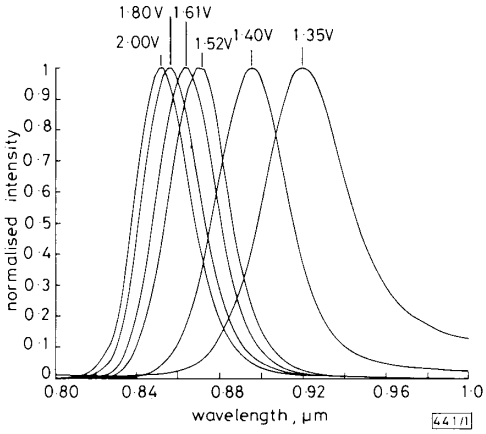

Fig. 1 *Output spectra of nipi LED at various applied voltages ($T = 77$ K)*

The rapid decrease in the rate of tuning above 120 K is similar to that observed by Döhler *et al.* in photoluminescence tuning in doping superlattices.[4] The temperature dependence of the tuning rate has been related to the competition between recombination by tunnelling and thermally activated recombination across the band-gap, and the critical temperature range related to the doping levels in the *p*- and *n*-layers. Of course, in an electroluminescent device there are additional limitations to the tuning such as self-heating due to series and contact resistances, and leakage currents. To clarify the temperature dependence of the EL in our devices, it was compared with the I/V characteristics in the range 80–300 K.

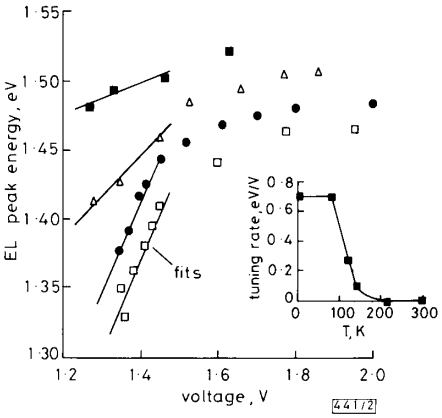

Fig. 2 *Tuning of electroluminescence against bias at various temperatures*

——— fits to determine tuning rate, which is plotted in inset
□ 3 K ● 77 K △ 123 K ■ 142 K

The I/V curves as functions of temperature are plotted for a current range of 10 nA–10 mA in Fig. 3. The results show distinct changes in the I/V characteristics as the temperature is increased. At temperatures lower than about 100 K the I/V curves show an exponential character over the part of the current range (from about 10 nA to 1 mA) where tunable luminescence is observed. Comparing the I/V characteristics with the EL tuning curves, that portion can be associated with recombination by tunnelling through the *nipi* potential barrier, resulting in tunable emission. The exponential factor in this region (applied bias <1·5 V) is ≈20·3, which may be interpreted as being characteristic of photon-assisted tunnelling in heavily doped *pn* junctions. For tunnelling by recombi-